Translational Oncology 13 (2020) 100744

Contents lists available at ScienceDirect

Translational Oncology

journal homepage: www.elsevier.com/locate/tranon

Inflammatory Infiltrate and Angiogenesis in Mantle Cell Lymphoma

Tiziana Annese [a], Giuseppe Ingravallo [b], Roberto Tamma [a], Michelina De Giorgis [a], Eugenio Maiorano [b], Tommasina Perrone [c], Francesco Albano [c], Giorgina Specchia [c], Domenico Ribatti [a,*]

[a] Department of Basic Medical Sciences, Neurosciences and Sensory Organs, Section of Human Anatomy and Histology, University of Bari Medical School Bari, Italy
[b] Department of Emergency and Organ Transplantation, Operating Unit of Pathological Anatomy, Aldo Moro University of Bari, Italy
[c] Department of Emergency and Organ Transplantation, Section of Hematology, University of Bari, Italy

ARTICLE INFO

Article history:
Received 18 December 2019
Received in revised form 21 January 2020
Accepted 21 January 2020
Available online xxxx

ABSTRACT

Mantle cell lymphoma (MCL) is an aggressive and rare B-cell non-Hodgkin lymphoma classified in two clinicopathological subtypes according to SOX11 expression and mutation state of immunoglobulin variable region heavy chain (IgVH) gene. The transcription factor SOX11, overexpressed in 78%-93% of MCL patients, plays a central role in modulating tumor microenvironment prosurvival signals and angiogenic genes. In this work, we have explored the lymph node microenvironment of three subgroups of MCL patients classified according to SOX11 expression as negative, light, and strong. $CD34^+$ microvessels, $CD4^+$ and $CD8^+$ T-lymphocytes, $CD68^+$ and $CD163^+$ macrophages, and the oncogene p53 expression were evaluated by immunohistochemistry. Moreover, STAT3 mRNA expression was analyzed by RNA-scope assay.

Our results confirmed increased angiogenesis in the sample of patients positive to SOX11 compared to the negative ones and demonstrated that angiogenesis and SOX11 expression positively correlate to a higher T-lymphocytes inflammatory infiltrate. On the contrary, angiogenesis and SOX11 expression negatively correlate with macrophage's inflammatory infiltrate and p53 expression. STAT3 mRNA expression level was not relevant concerning angiogenesis or SOX11 expression. Overall, our data indicate that, in MCL, SOX11 expression is associated with increased angiogenesis and a high $CD4^+$ and $CD8^+$ T-cell infiltration, which are not sustained by $CD163^+$ macrophages infiltrate and p53 expression.

Introduction

Mantle cell lymphoma (MCL) is an aggressive and rare B-cell non-Hodgkin lymphoma. It originates in the lymph nodes but frequently metastasizes in the bone marrow, spleen, and gastrointestinal tract, representing around 2%-10% of NHLs in adults [1,2]. MCL is predominantly found in men than in women at a ratio of 3:1, and the median age at diagnosis is 65 years old. It is associated with chromosomal translocation t(11;14)(q13;q32) in the naive pre-germinal center B-cells or with somatic mutations in the immunoglobulin variable region heavy chain (IgVH) gene resulting in upregulation of BCL-1 gene coding for protein cyclin D1 [3,4]. Although cyclin D1 overexpression is a hallmark of MCL, there is a patient subgroup which is cyclin D1 negative but presents cyclin D2/cyclin D3 translocations and SOX-11 overexpression with a similar genomic profile and clinical course to cyclin D1–positive MCL [5,6]. In the World Health Organization (WHO) 2016 update about lymphomas, based on clinical presentation and molecular mutations, two MCL main subtypes are distinguished: classical MCL or non-nodal MCL [7]. The first one is characterized by IgHV unmuted and SOX11 positivity leading to blastoid or pleomorphic types associated with an aggressive disease course. The second one is characterized by IgHV ipermuted and SOX11 negativity, and it is associated with an indolent disease course.

In addition to chromosomal aberration, MCL leads to considerable alterations in oncogenic genes such as p53, Notch1, CDKN2A, and ATM that are related to the angiogenic switch modulating thrombospondin-1, vascular endothelial growth factor, and hypoxia-inducible factor-1 [8–13]. Among these, p53 gene mutations and deletions are involved in MCL progression, and it appears to be a robust predictive biomarker for therapy failure [14]. Seventy percent of MCL patients are also signed by the constitutive activation of signal transducer and activator of transcription-3 (STAT3), as the result of an autocrine secretion of interleukin-6 and/or interleukin-10 (IL6 and/or -10) or in response to B-cell receptor engagement [15]. STAT3 acts as a repressor for SOX11 transcription by interacting directly with the SOX11 gene promoter and enhancer [16].

More than these intrinsic events and signals, also the extrinsic ones from the microenvironment contribute to MCL growth and progression. In lymphoid tissue, B-cells interact with different types of cells, such as stromal cells, macrophages, and T-cells, and are exposed to many

* Address all correspondence to: Domenico Ribatti, Department of Basic Medical Sciences, Neurosciences and Sensory Organs, Section of Human Anatomy and Histology, University of Bari Medical School Bari, Piazza Giulio Cesare 11, - 70124 Bari, Italy.
E-mail addresses: tiziana.annese@uniba.it, (T. Annese), giuseppe.ingravallo@uniba.it, (G. Ingravallo), roberto.tamma@uniba.it, (R. Tamma), michelina.degiorgis@uniba.it, (M. De Giorgis), eugenio.maiorano@uniba.it, (E. Maiorano), tommasina.perrone@uniba.it, (T. Perrone), francesco.albano@uniba.it, (F. Albano), giorgina.specchia@uniba.it, (G. Specchia), domenico.ribatti@uniba.it. (D. Ribatti).

http://dx.doi.org/10.1016/j.tranon.2020.100744

soluble factors belonging to the lymphoid microenvironment. The microenvironment components, if dysregulated, as during acute or chronic inflammation, can predispose or support tumorigenesis, which in turn supports the proinflammatory environment [17]. In these events, transcription factors and primary proinflammatory cytokines orchestrate the crosstalk between tumor cells and microenvironment, enhancing tumor cells proliferation and survival, neoangiogenesis mechanisms, metastasis processes, escape from adaptive immunity, drug resistance, accumulation of random genetic alterations in tumor cells, and inflammatory infiltrate recruitment [17]. In MCL, tumor cells could shape their microenvironment, activating a complex chemokine network to promote tumor progression, drug resistance development, and chemotherapy refractoriness [2]. In this context, SOX11 plays a central role in modulating tumor microenvironment prosurvival signals [18,19]. It has been well proven that SOX11 overexpressed in 78%-93% of MCL patients is associated with angiogenic genes upregulation and higher microvascular density compared with SOX11-negative MCL [20–22]. Furthermore, it has been shown that increased angiogenesis is associated with more aggressive behavior and a worse disease outcome [22]. Indeed, SOX11 overexpression promotes B-cell receptor (BCR) signaling, represses Bcl6 transcription and upregulates PAX5 to avoid B-cell differentiation into memory B-cells or plasma cells, promotes angiogenesis via platelet-derived growth factor A (PDGF-A), tumor cells homing and invasion via upregulation of (C-X-C motif) chemokine receptor 4 (CXCR4) and focal adhesion kinase (FAK) [18,21,23–25].

To date, the cellular composition of the microenvironment in MCL has not been systematically or definitively analyzed. In this work, we have explored the MCL microenvironment features evaluating $CD34^+$ microvessels, $CD4^+$ and $CD8^+$ T-lymphocytes, $CD68^+$ and $CD163^+$ macrophages, and the oncogene p53 according to SOX11 expression by immunohistochemistry (IHC). Moreover, we have analyzed STAT3 mRNA expression by RNA-scope assay.

Materials and Methods

Patients

Lymph node biopsies from 63 patients diagnosed with MCL were collected from the archive of the Section of Pathology of the University of Bari, Hospital Policlinico, Bari, Italy. All procedures were following the ethical standards of the responsible committee on human experimentation (institutional and national) and with the Helsinki Declaration of 1964 and later versions, and signed informed consent from individual patients was obtained to conduct the study.

MCL tissue sections have been processed for SOX11 IHC staining using a rabbit anti-SOX11 antibody at a dilution of 1:10 (Sigma-Aldrich, Darmstadt, Germany) (Figure 1). After counterstaining with Mayer's hematoxylin, the sections were evaluated by a certified pathologist (G.I.) who remained blinded to the clinical data using standard light microscopy.

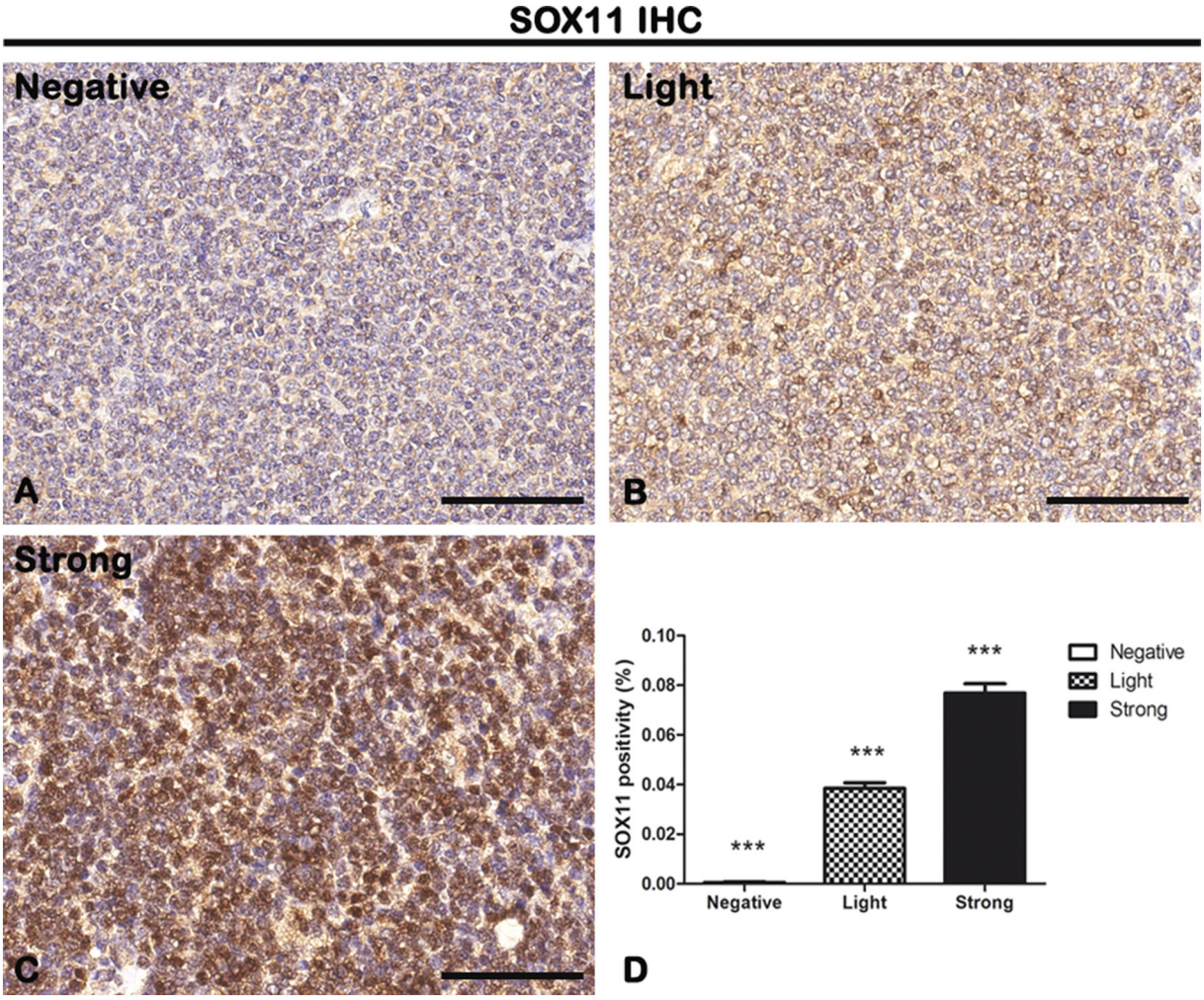

Figure 1. IHC of SOX11 on lymph node biopsies. Samples were divided into three histological groups based on the percentage of cells positive to SOX11 staining: negative group (0% of cells SOX^+) (A), light group (1%-39% of cells SOX^+) (B), or strong group ($\geq$ 40% of cells $SOX11^+$) (C). Morphometric analysis (D) shows a significative gradual increased SOX11 expression from negative to the strong group. Data are reported as means ± SD, and Bonferroni post-test was used to compare all groups after one-way ANOVA. Statistical significance: $***P \leq .001$. Scale bar: 80 μm.

Table 1
Antibodies Used for IHC

Protein	Catalog Number	Species	IHC Dilution	Antigen Retrieval	Source
SOX11	CLO143	Rabbit	1:10	Tris/EDTA pH 9	Sigma-Aldrich
CD34	QBEnd10	Mouse	1/500	Tris/EDTA pH 9	Beckman Coulter
CD4	4B12	Mouse	1:25	Tris/EDTA pH 9	Dako
CD8	ab75129	Mouse	Prediluted	Tris/EDTA pH 9	Abcam
CD68	ab125047	Rabbit	1:100	Tris/EDTA pH 9	Abcam
CD163	NCL-L-CD163	Mouse	1:300	Sodium citrate pH 6	Novocastra
p53	DO-7	Mouse	1:50	Sodium citrate pH 6	Dako
Anti-rabbit IgG	BA-1000	Goat	1:150		Vector Laboratories
Anti-mouse IgG	BA-9200	Goat	1:150		Vector Laboratories

Tumors samples were divided into three histological groups based on IHC SOX11 staining intensity positivity calculated by a semiquantitative scoring system: negative ($n = 20$) with no staining and 0% of cells positive to SOX11; light ($n = 25$) with a weak-moderate staining and 1%-39% of cells positive to SOX11; and strong ($n = 18$) with a moderate-strong staining and ≥40% of cells positive to SOX11. Moreover, the SOX11 staining was evaluated with the whole-slide scanning platform Aperio ScanScope as described below. Figure 1*D* shows the morphometric analysis of the SOX11 expression in negative (0.0005647% ± SD 0.0002707%), light (0.03845% ± SD 0.002292%), and strong (0.07690% ± SD 0.003692%) groups.

Immunohistochemistry

Archival formalin-fixed, paraffin-embedded human MCL histological sections of 2-μm thickness were collected on poly-L-lysine–coated slides, deparaffinized, and rehydrated in a xylene-graded alcohol scale and then rinsed in Tris-buffered saline solution (TBS). For antigen retrieval, the sections were heated in a solution of sodium citrate pH 6.0 or Tris/EDTA buffer pH 9 (cod. S1699 or cod. S2367, Agilent Dako, Santa Clara, CA) once the temperature has reached 98°C in a water bath for 20 minutes (Table 1), and after three washes in TBS + 0.025 Triton X-100, the slides were left in a blocking buffer [BB; TBS pH 7.4

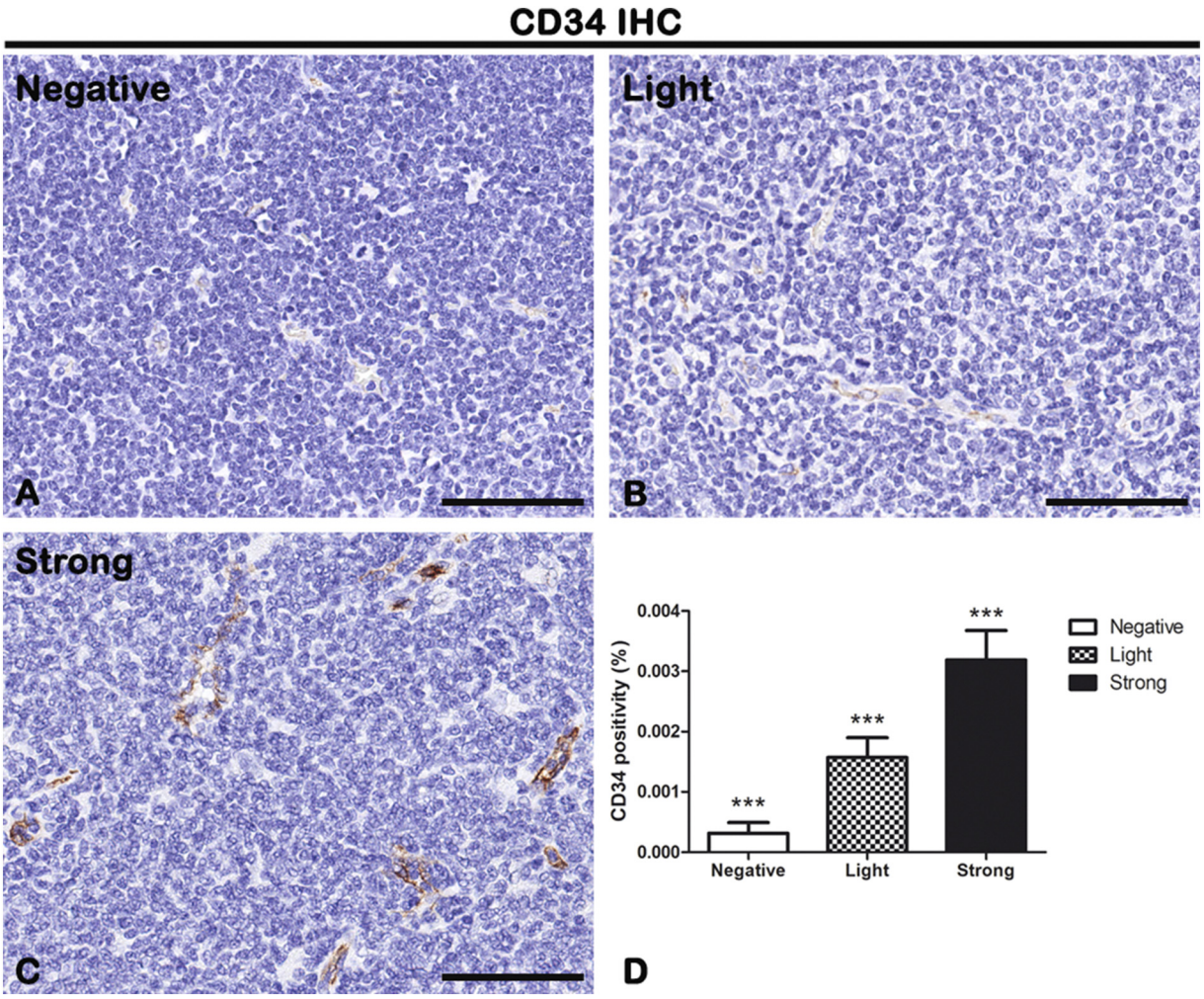

Figure 2. IHC of endothelial cells marker CD34 on lymph node biopsies of negative (A), light (B), and strong (C) groups classified according to SOX11 staining intensity. Morphometric analysis (D) shows a significative gradual increased CD34 expression from negative to the strong group. Data are reported as means ± SD, and Bonferroni post-test was used to compare all groups after one-way ANOVA. Statistical significance: ***$P \leq .001$. Scale bar: 80 μm.

+ 1% bovine serum albumin (BSA) + 10% normal goat serum] for 2 hours. Subsequently, the sections were incubated with primary unconjugated antibodies (Table 1) diluted in TBS + 1% BSA overnight at 4°C and washed in TBS + 0.025 Triton X-100, and endogenous peroxidases were blocked using 3% hydrogen peroxide solution for 10 minutes in the dark. Then, the sections were incubated with biotinylated goat anti-rabbit IgG or goat anti-mouse IgG diluted in TBS + 1% BSA for 1 hour followed by streptavidin-peroxidase conjugate (cod. A-2704, Vector Laboratories) for 30 minutes. Finally, the immunodetection was performed in distillate water with AEC or DAB substrate kit for peroxidase (cod. SK-4200 or cod. SK-4100, Vector Laboratories) for 40 minutes per AEC and 2 minutes per DAB at room temperature. Finally, the sections were counterstained with Mayer's hematoxylin (cod. 51275, Sigma-Aldrich, St. Louis, MO) and mounted in glycergel (cod. C0563, Agilent Dako). Specific preimmune serum replacing the primaries antibodies served as a negative control.

Morphometric Analysis

All slides were scanned at the maximum magnification available (40×) using the whole-slide scanning platform Aperio ScanScope CS (Leica Biosystems, Nussloch, Germany) and were viewed and analyzed remotely employing Positive Pixel Count algorithm embedded in the ImageScope v.11.2.0.780 (Leica Biosystems). Using this algorithm, each immunohistochemical signal was individually calibrated to calculate the number of strong positive pixels, the number of medium positive pixels, and the number of weak positive pixels. The positivity value results, calculated as the total number of positive pixels divided by the total number of pixels, were considered.

RNAscope Analysis

RNA *in situ* hybridization was performed using RNAscope® 2.5 HD Reagent Kit [RED 322360, Advanced Cell Diagnostics, Hayward, CA] as described [26]. Briefly, deparaffinized tissue sections were hybridized with the Hs-STAT3 probe (ref. 425631), positive control probe Hs-PPIB (ref. 313901), or negative control probe DapB (ref. 310043) at 40°C for 2 hours. After hybridizations, sections were subjected to signal amplification, Gill's hematoxylin counterstaining, and scanning (Aperio ScanScope CS, Leica Biosystems, Nussloch, Germany) at 40× magnification. Fast Red semiquantitative image analysis was performed using the Aperio RNA ISH algorithm, which automatically quantifies the staining across whole slides and counts individual molecular signals and clusters in the cells. The obtained results are divided into three ranges: 1, which includes cells containing 2-5 dots per cell; 2, which includes cells containing 6-20 dots per cell; and 3, which includes cells containing more than 20 dots per cell.

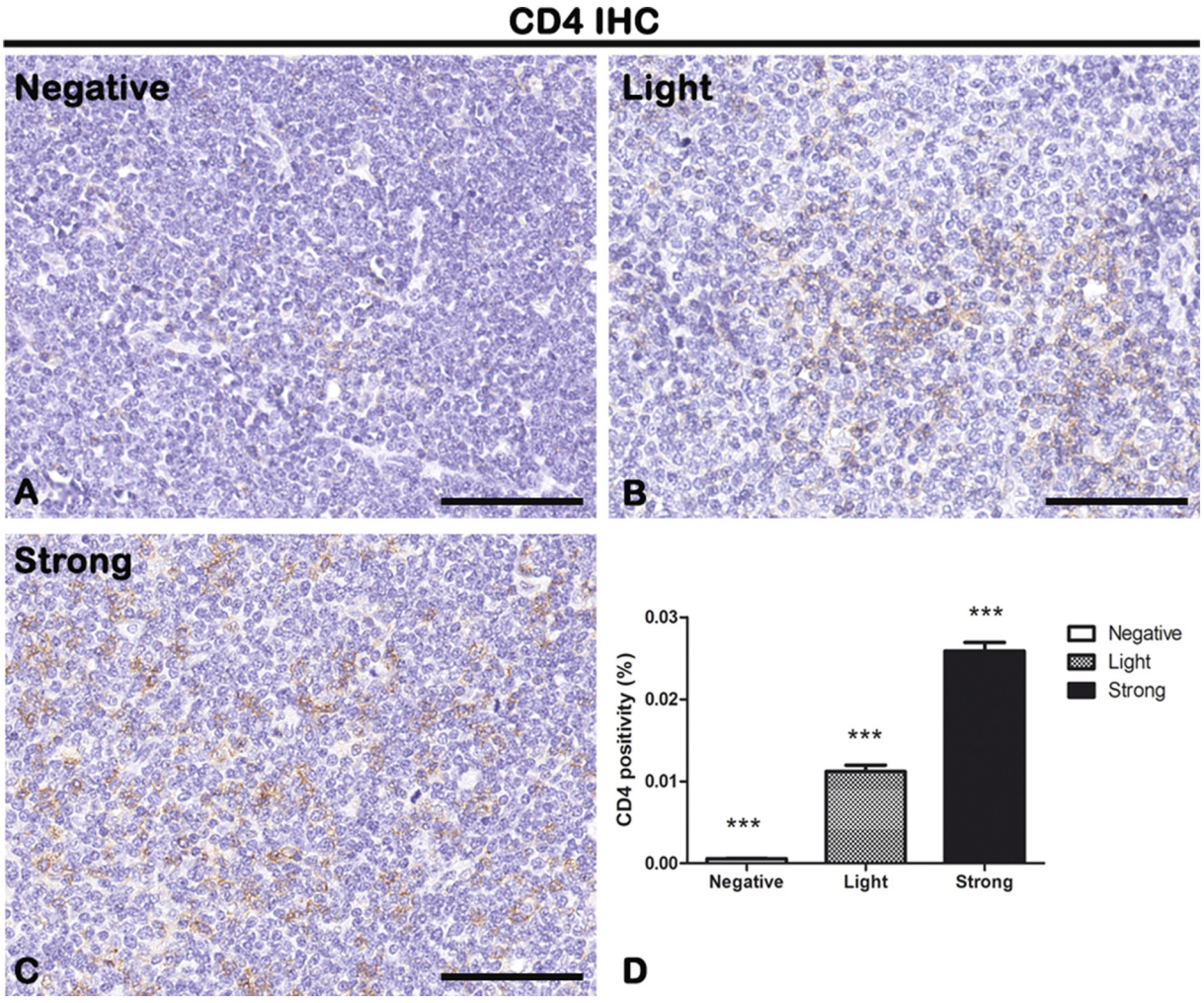

Figure 3. IHC of T-lymphocytes marker CD4 on lymph node biopsies of negative (A), light (B), and strong (C) groups classified according to SOX11 staining intensity. Morphometric analysis (D) shows a significative increase in CD4 expression from negative to strong groups. Data are reported as means ± SD, and Bonferroni post-test was used to compare all groups after one-way ANOVA. Statistical significance: ** $P \leq .01$; *** $P \leq .001$. Scale bar: 80 μm.

Statistical Analysis

One-way ANOVA with Bonferroni post hoc tests and Spearman non-parametric correlation analysis were performed using GraphPad Prism 5.01 statistic package (GraphPad Software, San Diego, CA). Statistical significance was set at $P \leq .05$, and results are given as mean ± SD.

Results

Angiogenesis and SOX11 Expression Positively Correlate to T-Lymphocytes Inflammatory Infiltrate

CD34, CD4, and CD8 IHC reactions were performed on lymph node biopsies of negative, light, and strong groups, classified according to SOX11 staining intensity (Figure 1), to evaluate neoangiogenesis mechanisms (Figure 2 for CD34) and the presence of $CD4^+$ and $CD8^+$ T-lymphocytes (Figures 3 and 4) in mantle cells lymphoma.

As shown in Figure 2, in light and strong groups, the blood vessels are positive to the endothelial and hematopoietic stem cell marker CD34, which does not seem to be present in the negative one (Figure 2). Figure 2*D* shows the morphometric analysis of the CD34 expression in negative (0.0003161% ± SD 0.0001771%), light (0.001572% ± SD 0.0003269%), and strong (0.003188% ± SD 0.0004868%) groups. The correlation study proves a positive one between CD34 and SOX11 ($r = 0.8593$, $P \leq .0001$ with SOX11; Figure 10). Therefore, these results demonstrate that SOX11 may promote new blood vessels formation in MCL, as already mentioned by others, via sprouting angiogenesis and vasculogenesis [22,24,27,28].

The cytotypes most present in the inflammatory infiltrate of MCL lymph nodes are the T-lymphocytes, as shown in Figures 3 and 4. Figure 3*D* shows the morphometric analysis of the CD4 expression in negative (0.0005648% ± SD 0.0001931%), light (0.0119% ± SD 0.003822%), and strong (0.02589% ± SD 0.004348%) groups. Figure 4*D* shows the morphometric analysis of the CD8 expression in negative (0.01715% ± SD 0.0006553%), light (0.02557% ± SD 0.001759%), and strong (0.03385% ± SD 0.002333%) groups. $CD4^+$ and $CD8^+$ T-lymphocytes are present in all the groups, and a gradual and statistical significative increase is evident from negative to strong SOX11-positive group, as confirmed by the correlation study between CD4 or CD8 and CD34 or SOX11 expression (for CD4: $r = 0,.8399$, $P \leq .0001$ with CD34; $r = 0.9165$, $P \leq .0001$ with SOX11; for CD8: $r = 0.9144$, $P \leq .0001$ with CD34; $r = 0.8453$, $P \leq .0001$ with SOX11; Figures 9 and 10). Taken together, these results confirm a close positive correlation between neoangiogenesis mechanisms activation and SOX11 expression supported by higher CD4 and CD8 positive T-lymphocytes inflammatory infiltrate in the $SOX11^+$ strong group. These T-cells are probably involved in the formation of an immunosuppressive microenvironment that promotes tumor escape from the patient's immune system.

Angiogenesis and SOX11 Expression Negatively Correlate with Macrophages Inflammatory Infiltrate and p53 Expression

CD68, CD163, and p53 IHC reactions were performed on lymph node biopsies of negative, light, and strong groups, classified according to SOX11 staining intensity, to characterize macrophage inflammatory infiltrate (Figures 5 and 6 for CD68 and CD163, respectively) and the

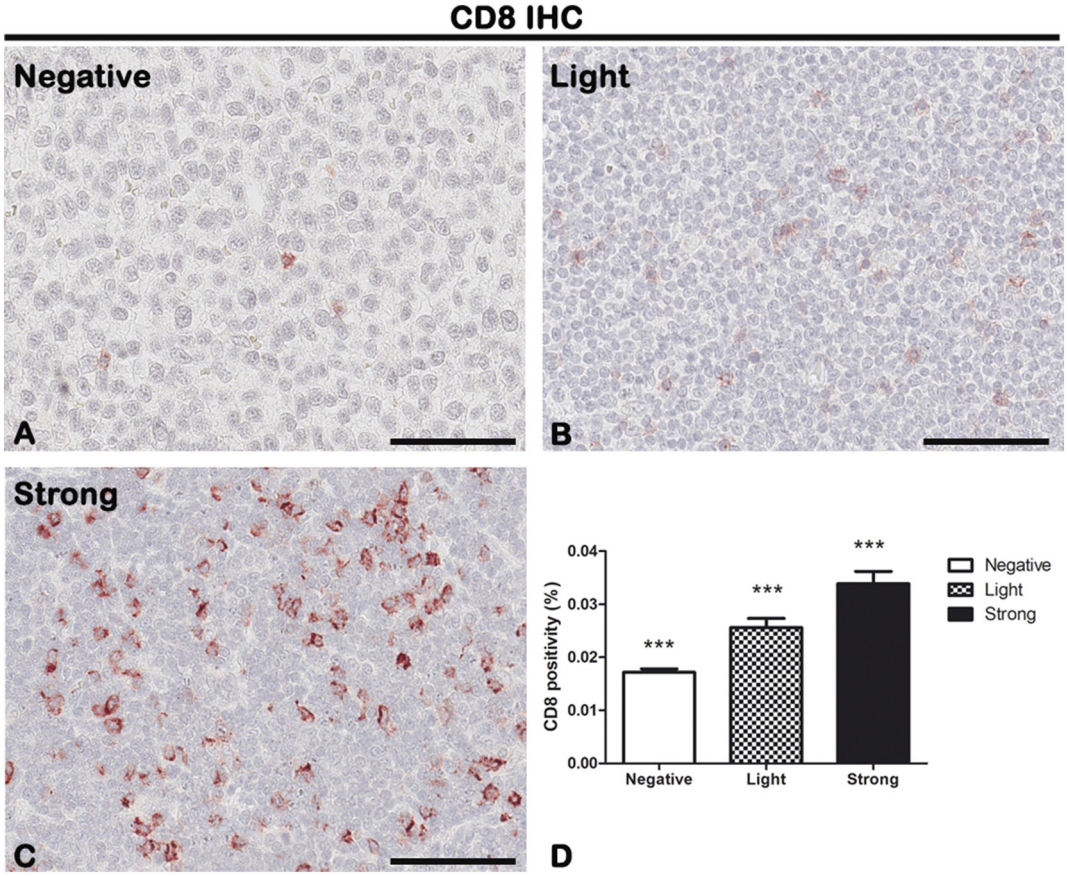

Figure 4. IHC of T-lymphocytes marker CD8 on lymph node biopsies of negative (A), light (B), and strong (C) groups classified according to SOX11 staining intensity. Morphometric analysis (D) shows a significative gradual increased CD8 expression from negative to the strong group. Data are reported as means ± SD, and Bonferroni post-test was used to compare all groups after one-way ANOVA. Statistical significance: ***$P \leq .001$. Scale bar: 80 μm.

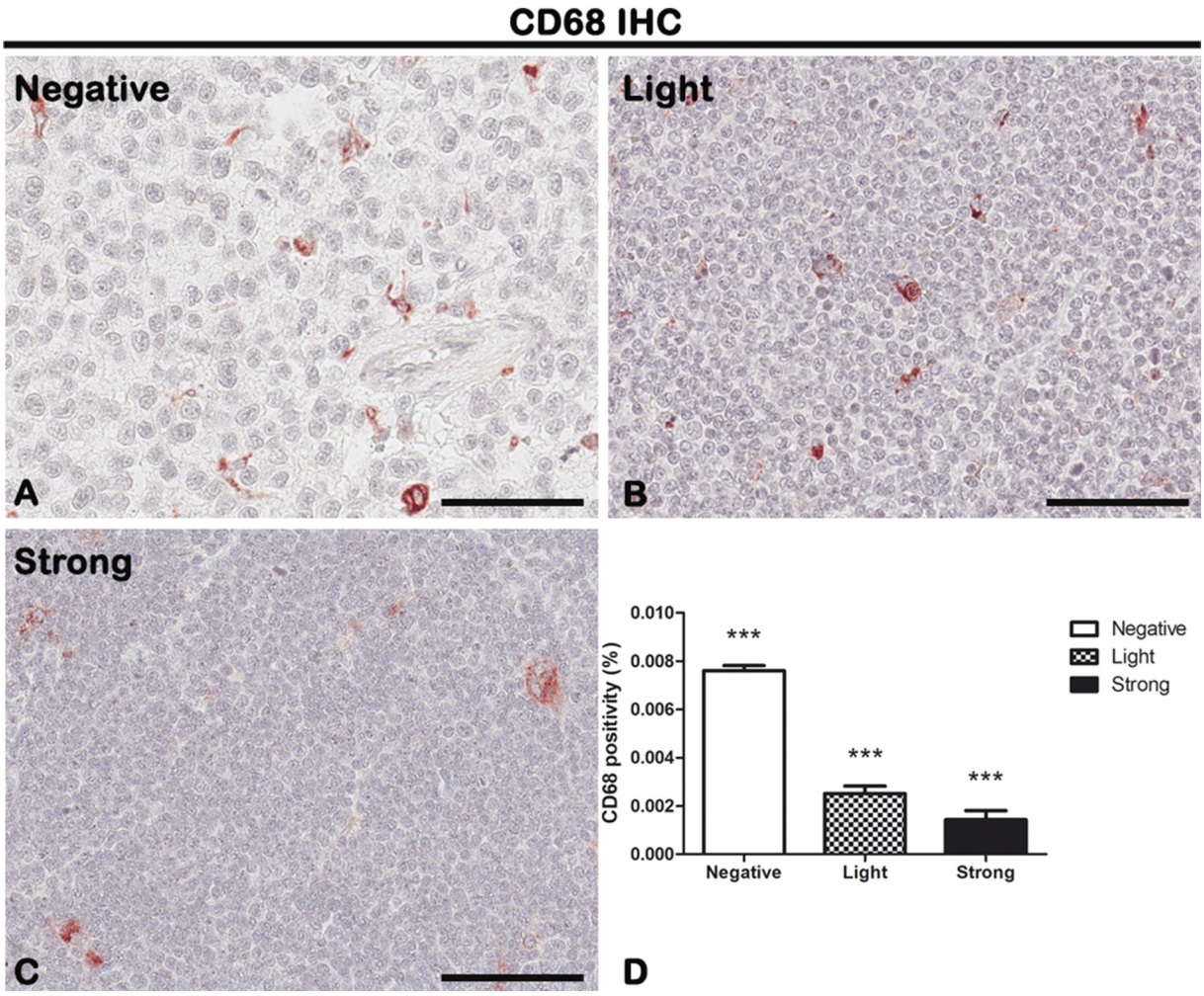

Figure 5. IHC of pan-macrophage marker CD68 on lymph node biopsies of negative (A), light (B), and strong (C) groups classified according to SOX11 staining intensity. Morphometric analysis (D) shows a significative gradual decrease in CD68 expression from negative to the strong group. Data are reported as means ± SD, and Bonferroni post-test was used to compare all groups after one-way ANOVA. Statistical significance: ***$P \leq .001$. Scale bar: 80 μm.

expression of oncogene p53 (Figure 7) in mantle cells lymphoma. As shown in Figures 5 and 6, $CD68^+$ and $CD163^+$ macrophages are present in all the groups. Figure 5*D* shows the morphometric analysis of the CD68 expression in negative (0.007608% ± SD 0.0002004%), light (0.002516% ± SD 0.0003026%), and strong (0.001431% ± SD 0.0003725%) groups. Figure 6*D* shows the morphometric analysis of the CD163 expression in negative (0.01491% ± SD 0.002147%), light (0.006889% ± SD 0.001949%), and strong (0.0007801% ± SD 0.0003464%) groups. The correlation study between CD68 or CD163 and CD34 or SOX11 expression has shown a gradual and statistically significative decrease from negative to strong SOX11 positive group (for CD68: $r = -0.8774$, $P \leq .0001$ with CD34; $r = -0.8800$, $P \leq .0001$ with SOX11; for CD163: $r = -0.8774$, $P \leq .0001$ with CD34; $r = -0.8617$, $P \leq .0001$ with SOX11; Figures 9 and 10). Unlike $CD68^+$ macrophages that have a mostly rounded shape and are distributed also within the tumor mass (Figure 5), the $CD163^+$ rounded ones are preferentially accumulated in peripheral connective tissue in negative and light group compared to strong one, whereas $CD163^+$ macrophages with elongated shapes are present within the tumor mass in all the three groups (Figure 6). Figure 7 shows a very modest positivity for p53 in all the samples, but a gradual and statistically significative decrease is evident from negative to strong SOX11 positive group, as confirmed by the correlation study on the relationship between p53 and CD34 or SOX11 expression in the three groups ($r = -0.8695$, $P \leq .0001$ with CD34; $r = -0.8544$, $P \leq$ 0,0001 with SOX11; Figures 9 and 10). Figure 7*D* shows the morphometric analysis of the p53 expression in negative (0.0006469% ± SD 0.0001393%), light (0.0001570% ± SD 0.00004547%), and strong (0.00003809% ± SD 0.00003092%) groups. Taken together, these results reveal a close negative correlation among neoangiogenesis mechanisms activation and SOX11 expression with both macrophages inflammatory infiltrate and p53 expression.

STAT3 mRNA Expression Is Not Related to Angiogenesis or SOX11 Expression

RNAscope in situ hybridization to STAT3 mRNA evaluation was performed on lymph node biopsies of negative, light, and strong groups, classified according to SOX11 staining intensity (Figure 8). The pictures in Figure 8 show that STAT3, like red spots, is expressed in all the groups but the quantification analysis, performed by Aperio RNA ISH algorithm, dividing data into three groups according to number of spots per cell (Figure 8*D*) or cellular localization (Figure 8*E*), did not indicate any relevant difference ($P > .05$). In negative/group 0+ (60.27% ± SD 9.77%), negative/group 1+ (40.30% ± SD 7.38%), negative/group 2+ (1.15% ± SD 0.43%), negative/in cells (0.74% ± SD 0.23%), negative/in nuclei (0.20% ± SD 0.09%), negative/in cytoplasm (0.55% ± SD 0.14%), as compared to light/group 0+ (63.13% ± SD 7.31%), light/group 1+ (38.59% ± SD 7.50%), light/group 2+ (1.01% ± SD 0.67%), light/in cells (63.13%

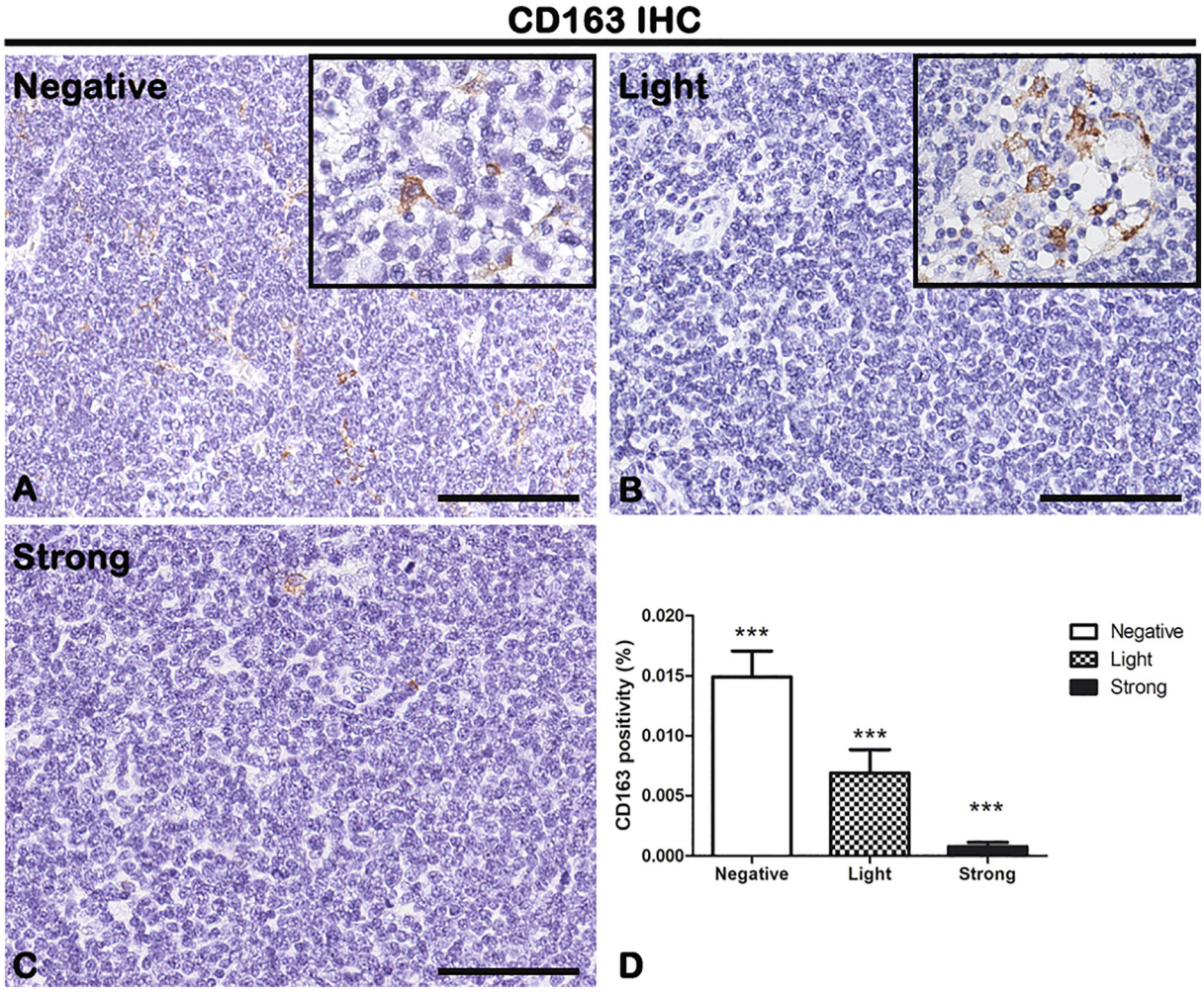

Figure 6. IHC of M2 macrophage marker CD163 on lymph node biopsies of negative (A), light (B), and strong (C) groups classified according to SOX11 staining intensity. Inserts in A and B show round and larger macrophages present in few areas of the samples. Morphometric analysis (D) shows a significative gradual decreased CD163 expression from negative to the strong group. Data are reported as means ± SD, and Bonferroni post-test was used to compare all groups after one-way ANOVA. Statistical significance: ***$P \leq .001$. Scale bar: 80 μm.

± SD 0.23%), light/in nuclei (38.53% ± SD 0.08%), light/in cytoplasm (1.01% ± SD 0.15%), as compared to strong/group 0+ (5374% ± SD 6.63%), strong/group 1+ (42.41% ± SD 5.29%), strong/group 2+ (2.33% ± SD 0.64%), strong/in cells (53.74% ± SD 0.17%), strong/in nuclei (42.41% ± SD 0.09%), strong/in cytoplasm (2.33% ± SD 0.13%).

These results demonstrate that the constitutive activation of STAT3 in MCL is not related to an increased gene expression but probably to other mechanisms related to protein stability or mRNA degradation [15,29].

Discussion

MCL is an aggressive B-cell NHL with poor long-term survival. MCL patients are first diagnosed at an advanced stage, typically with the involvement of the lymph nodes, bone marrow, spleen, and gastrointestinal tract [30,31]. Today, there is no specific care for the treatment of MCL because of its high heterogeneity. Thanks to the growing knowledge of its biology, ontogeny, and molecular pathology, two main clinicopathological subtypes of MCL are recognized [7]. The first subtype is named classical MCL and is characterized by IgHV gene unmuted and SOX11 positivity, leading to blastoid or pleomorphic types associated with an aggressive disease course. The second one is named non-nodal MCL and is characterized by IgHV gene ipermuted and SOX11 negativity, and it is associated with an indolent disease course. Although the prognostic role of SOX11 is controversial because others have shown that most indolent MCLs are SOX11$^+$ [32]. In general, SOX11 is specifically expressed in MCL compared with other lymphomas, and in nonmalignant bone marrow, no evidence of nuclear SOX11 staining was found [5,33]. In MCL, the staining of SOX11 is nuclear, intense, and present in the majority of the tumor cells [5].

A combination of aberrant cell cycle regulation, DNA damage, molecular and genomic alterations, BCR signaling, and interactions with the lymphoid tissue microenvironment forms the basis of MCL cell growth.

The role of the lymphoid tissue microenvironment in MCL progression is not still fully understood. Therefore, in this study, we provide an in-depth evaluation of immune-inflammatory cells and blood microvessels using the high-throughput morphology analysis by Aperio ScanScope CS. The microenvironment elements could protect against tumorigenesis and invasion if it is in a healthy state, or it could be a "partner in crime" promoting tumor initiation, progression, and metastasis if it is not in a healthy state [34]. The microenvironment consists of extracellular matrix macromolecules, myofibroblasts, fibroblasts, neuroendocrine cells, adipose cells, immune-inflammatory cells, and the blood and lymphatic vessels [35]. In MCL, these elements provide extrinsic signals to tumor cells, activate prosurvival signaling like BCR and classical and alternative NF-kB

pathways, and sustain the imbalance of the Bcl-2 family downregulating Bim and inducing Bcl-xL [2].

In many lymphoid tumors, the association between increased angiogenesis and more aggressive behavior featured by increased tumor proliferation and dissemination has been suggested [36,37]. In this study, by CD34 IHC reaction, we have demonstrated and confirmed that neoangiogenesis mechanisms occur in MCL with negative, light, or strong SOX11 expression, and in the latter, it is much more than the first two. Furthermore, we have shown a close positive correlation between CD34 and SOX11 expression. These results are in accord with others that compare intratumoral microvascular density and area in SOX11-positive and -negative MCL patients using CD34 staining [38]. They have been showed that, in SOX11-negative MCL, there is a corona-like distribution of blood vessels in the stroma surrounding the nodules indicating a less invasive tumor phenotype compared to the SOX11-positive one, where the blood vessels were randomly distributed [22]. Moreover, CD34 positivity could be considered a sign of neoangiogenesis mechanisms activation as it has been identified as tip cell-specific markers by whole genome genetic profiling strategies [27,39].

Comparing MCL patients negative to SOX11 expression with those moderately positive to it (1%-39% of cells positive to SOX11) and with those strongly positive to it (40%-100% of cells positive to SOX11), our results have shown a significant difference in microenvironment composition about lymphocytes and macrophage infiltration, and p53 expression according to SOX11 level.

We have demonstrated a higher $CD4^+$ and $CD8^+$ T-lymphocytes inflammatory infiltrate in MCL lymph node biopsies of patient"s strong group, that positively correlate with strong SOX11 intensity and increased angiogenesis, compared with the other ones. Usually, $CD4^+$ and $CD8^+$ T-cells induce immune responses against tumors. In fact, analyzing the peripheral blood and lymph nodes of MCL patients, it was demonstrated that $CD4^+$ and $CD8^+$ T-cells are lower in aggressive forms of MCL and a low CD4:CD8 ratio is a predictor of unfavorable overall survival [40,41]. Our results do not agree with this, probably because we did the inflammatory infiltrate evaluation concerning SOX11 expression and not clinical outcome. Alternatively, a more detailed T-cell phenotypic characterization could lead to the identification of a specific CD4-positive T-cell subset like Th1, Th2, Th9, Th17, Th22, and Tfh, with a role in the inhibition of antitumor immune response [42]. For example, the immunosuppressive Tregs cells ($CD4^+CD25^+FoxP3^+$), whose increase correlates with advanced tumor growth and predicts poor prognosis, could be much more in MCL patients with higher SOX11 expression [43]. Otherwise, as demonstrated in chronic lymphocytic leukemia, $CD4^+$ T-cells could have a Th2 cell profile that supports tumor cells via cytokines, chemokines, and membrane receptors [44]. The increased number of cytotoxic $CD8^+$ T-lymphocytes in the strong group, which is the one with the worse outcome, compared to the negative and light ones, which have a favorable prognosis, could be related to the activation of tumor immune evasion processes. It was demonstrated that $CD8^+$ T-cells promote the secretion of prostaglandin E2 by tumor cells

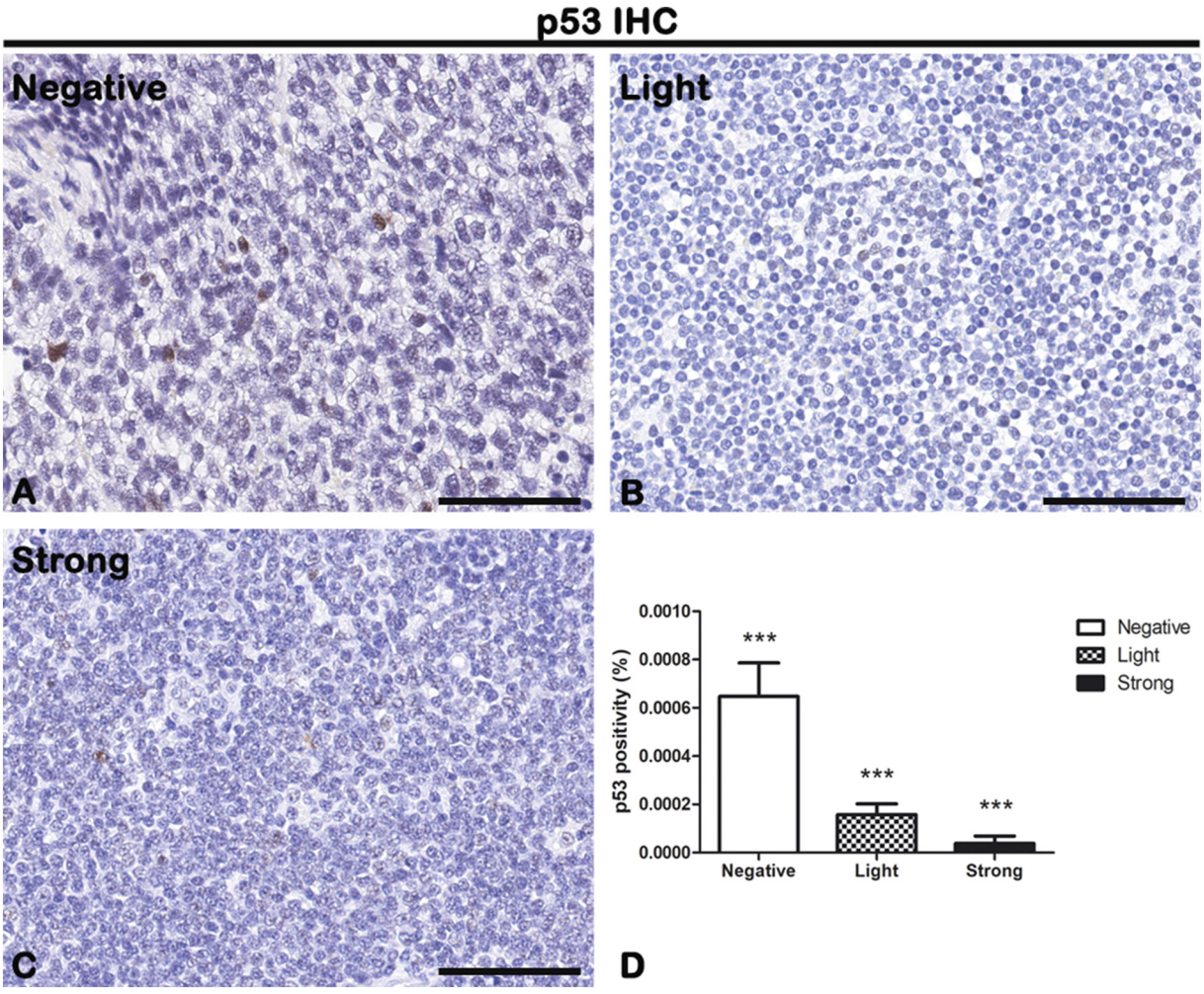

Figure 7. IHC of the cellular tumor antigen p53 on lymph node biopsies of negative (A), light (B), and strong (C) groups classified according to SOX11 staining intensity. Morphometric analysis (D) shows a significative gradual decreased p53 expression from negative to the strong group. Data are reported as means ± SD, and Bonferroni post-test was used to compare all groups after one-way ANOVA. Statistical significance: ***$P \leq .001$. Scale bar: 80 μm.

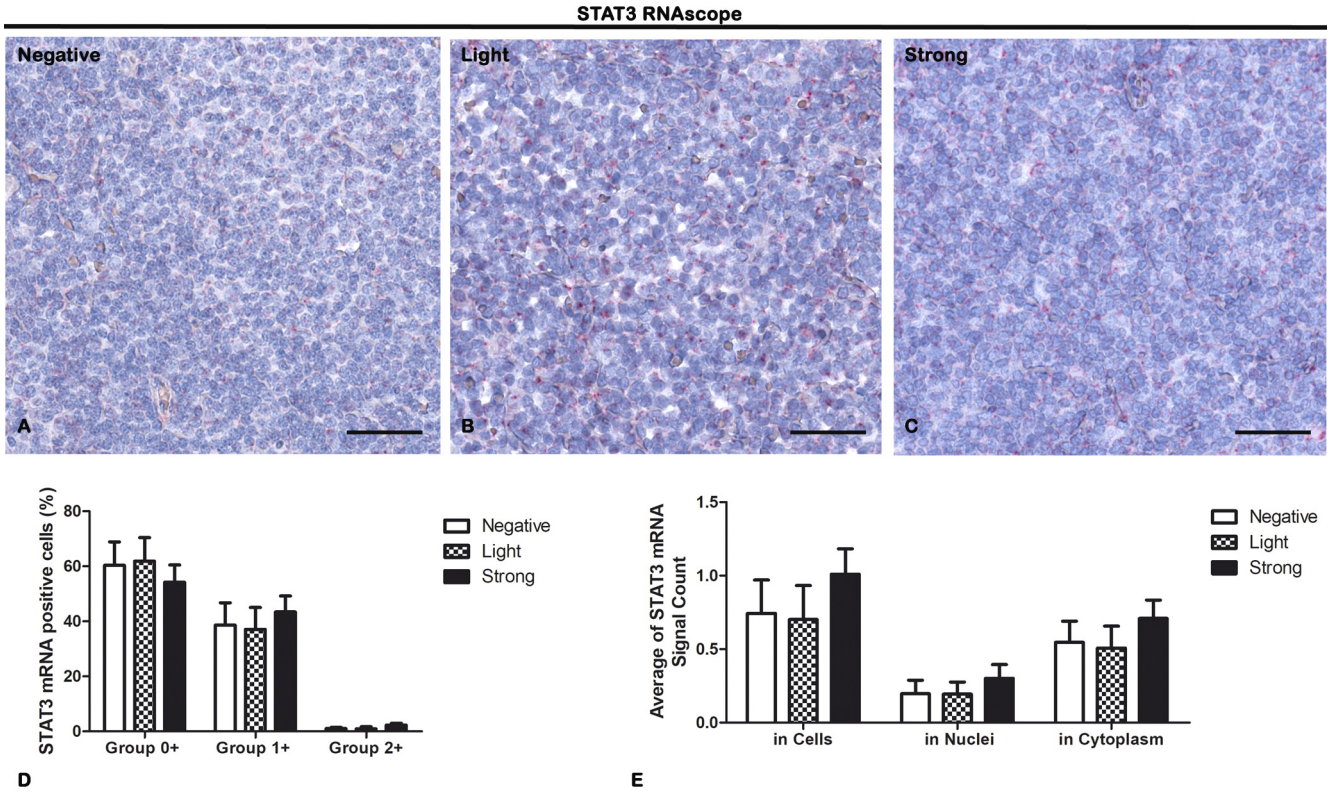

Figure 8. RNAscope in situ hybridization of STAT3 on lymph node biopsies of negative (A), light (B), and strong (C) groups classified according to SOX11 staining intensity. Morphometric analyses (D, E) show STAT3 mRNA expression in all the samples without any significant difference among the groups both in number of dots per cell and in cellular localization (D). Data are reported as means ± SD, and Bonferroni post-test was used to compare all groups after one-way ANOVA. Statistical significance: no. Scale bar: 80 μm.

and increase the myeloid-derived suppressor cells recruitment via Fas signaling causing tumor escape [45,46]. Moreover, the Fas/FasL signaling promotes the expression of proinflammatory chemokines and angiogenesis as demonstrated in malignant astrocytoma [47].

Our results have shown reduced $CD68^+$ and $CD163^+$ macrophages inflammatory infiltrate in MCL lymph node biopsies of patient's strong group compared to the other two that inversely correlates with increased SOX11 intensity and angiogenesis. In all groups, $CD163^+$ cells usually outnumbered $CD68^+$ cells and presented both rounded and elongated shapes. Monocytes/macrophages can promote angiogenesis, suppress antitumor immunity, and drive the survival of lymphoma cells [48,49]. In most tumors, an inflammatory infiltrate rich in macrophages is associated with a more aggressive phenotype and with a higher proliferation rate, and negatively correlates with overall survival [48]. Two main macrophage subpopulations could be distinguished using molecular markers and cytokine secretion profile: the proinflammatory M1 macrophages, promoting Th1 responses and showing tumoricidal activity, and the anti-inflammatory M2 macrophages, contributing to tissue repair and promoting Th2 responses. CD68 is usually used to identify all the macrophages, but CD163 is considered an M2 marker [50]. However, it is a controversial issue if all $CD163^+$ cells are M2 macrophages [51]. Moreover, M1 macrophages are usually characterized by the classical pancake-like shape that could be changed according to their function [52]. It was demonstrated that proinflammatory M1 could take an elongated shape, which is strictly correlated to an anti-inflammatory M2 phenotype transition, by applying an external mechanical force on already differentiated macrophages or by blocking HDAC activity [53]. *In vitro* under IL-10 and CSF1 stimuli, it was demonstrated that MCL monocytes polarize into M2-like macrophages, which in turn favor tumor survival and proliferation [49]. Regarding angiogenesis, it was suggested that M1 macrophages induce sprouting angiogenesis, while M2 macrophages are involved in blood vessel stabilization via pericyte recruitment [54]. Therefore, our results have shown a mixed M1/M2 population, where $CD163^+$ rounded and elongated macrophages are mostly present in groups of patients with negative or low expression of SOX11, highlighting their marginal role in the maintenance of a protumorigenic microenvironment in SOX11-positive patients.

p53 IHC analysis has shown a gradual content decrease, from negative to strong SOX11-positive group, with a general low expression in all the three groups compared to the other proteins analyzed. Furthermore, we found that p53 expression negatively correlates with strong SOX11 intensity and increased angiogenesis. In agreement with us, it was demonstrated that p53 status has a good correlation with negative/low SOX11 mRNA levels in both non-nodal and classical mantle cell lymphoma [55,56]. p53 is the most common oncogene associated with human cancer. It is on chromosome 17 and, in the case of DNA damages, acts as a negative/positive regulator of cell proliferation/apoptosis, respectively. Its alterations identify a high-risk population signed by reduced sensitivity to conventional chemotherapy with cytarabine and rituximab at high dose, followed by consolidation therapy with autologous stem cell transplantation [54]. Noteworthy is the role of p53 as an inhibitor of inflammatory responses and of somatic cells reprogramming to stem cells during inflammation. However, in tumor, the functional loss of p53 fail to maintain suppressive microenvironment causing excessive inflammatory reactions that in turn sustain tumor growth and progression [57].

The RNAscope assay performed to evaluate STAT3 mRNA expression in lymph node biopsies of MCL patients did not show any significant difference in its expression amount or cellular localization among the three groups. In MCL, STAT3 is constitutively activated and acts as a repressor decreasing SOX11 expression [16,58]. Contrary to what has been shown in other lymphomas, our results have demonstrated that the constitutive

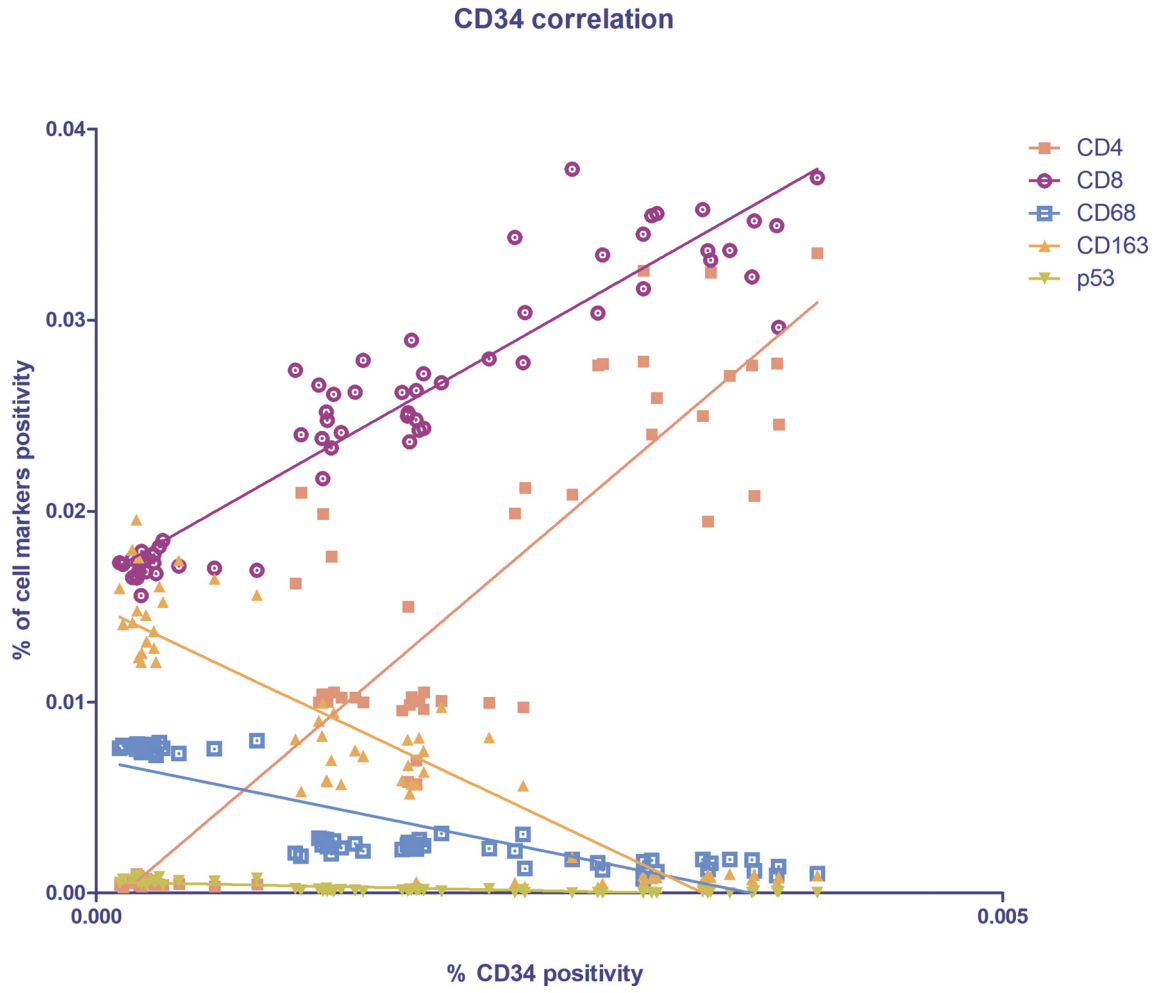

Figure 9. Spearman's correlation graph between CD34 (*x*-axis) and the inflammatory infiltrate cell markers (*y*-axis) positivity on lymph node biopsies. Statistical significance was determined by linear regression analysis ($P \leq .0001$).

activation of STAT3 in MCL is not related to an increased gene expression but probably to other mechanisms related to protein stability or mRNA degradation [26,29]. The link between tumor microenvironment, signed by the inflammatory infiltrate, and MCL, signed by SOX11 overexpression and STAT3 constitutive activation, could be represented by IL-6. MCL cells and inflammatory infiltrate cells can secrete IL-6 and its soluble receptor gp80 promoting, in an autocrine and paracrine mode, MCL survival, growth, and drug resistance [59].

These results suggest that SOX11 promotes a tumor protective microenvironment supporting MCL progression and immune escape. Accordingly, it was demonstrated that the pathways CXCR4/CXCL12 and FAK/PI3K/AKT play a significant role in MCL-microenvironment crosstalk contributing to a more aggressive phenotype and worse outcome [18,60]. SOX11 directly binds to regulatory regions of genes encoding for CXCR4 and FAK and activating the FAK/PI3K/AKT pathway promoting higher tumor cells homing and invasion, and increases cell adhesion–mediated drug resistance in positive MCL patients compared with the negative ones [18]. FAK is highly expressed in bone marrow infiltrates of MCL, and its stroma-mediated activation leads to the activation of multiple kinases involved in prosurvival and proliferation signaling causing secondary mechanisms of drug resistance [60]. In fact, it was demonstrated that FAK, with other acquired mechanisms of resistance, induces resistance to ibrutinib, a small molecule inhibitor of Bruton tyrosine kinase applied in relapsed or refractory MCL [60]. Therefore, new therapeutical approaches that destroy the tumor-stromal protective microenvironment and tumorigenic B-cell by immunochemotherapy depletion are emerging as a promising strategy for the treatment of MCL [61,62].

Conclusions

In conclusion, our results have shown, in MCL, different immune-inflammatory cells and blood microvessels composition concerning SOX11 expression. The high SOX11 positivity (40%-100% of lymph node cells) is associated with increased angiogenesis and a high $CD4^+$ and $CD8^+$ T-cell infiltration, which are not sustained by $CD163^+$ macrophages infiltrate and p53 expression. On the contrary, the tumor proliferation and progression in MCL patients negative to SOX11 are sustained by $CD163^+$ macrophages infiltrate and p53 expression. An intermediate microenvironment composition features the patients with low SOX11 expression.

The identification of peculiar characteristics that can allow distinguishing the microenvironment composition in MCL concerning SOX11 expression is complex, and even more complicated is to determine the individual contribution of all microenvironment components to the tumor behavior. Microenvironment comparative analysis in larger cohorts of patients with high-throughput molecular and morphology analysis is indispensable to understand better the mechanisms underlying MCL pathogenesis. Future therapeutic approaches will have to consider the disruption of crosstalk between the tumor cells and their microenvironment, such as adding B-cell receptor pathway inhibitors, lenalidomide, or proteasome inhibitors [55].

Acknowledgements

This work was supported by Associazione “Il Sorriso di Antonio,” Corato, and Associazione Italiana Contro le Leucemie, Linfomi e Mielomi (AIL), Bari, Italy.

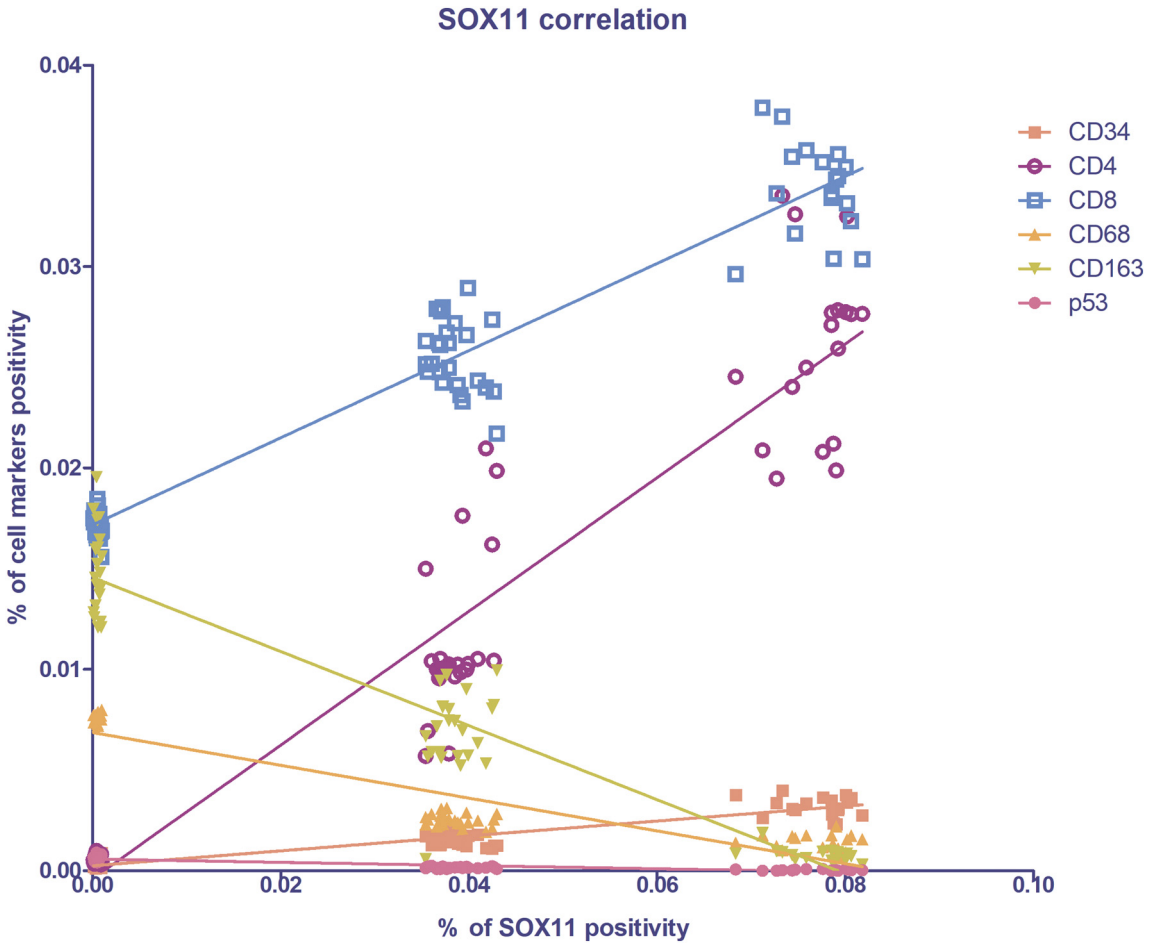

Figure 10. Spearman's correlation graph between SOX11 (*x*-axis), endothelial and the inflammatory infiltrate cell markers (*y*-axis) positivity on lymph node biopsies. Statistical significance was determined by linear regression analysis ($P \leq .0001$).

Conflicts of Interest

The authors declare that they have no conflicts of interest with the contents of this article.

Funding

This research did not receive any specific grant from funding agencies in the public, commercial, or not-for-profit sectors.

References

[1] Lynch DT and Acharya U (2019). Cancer. mantle cell lymphoma. Treasure Island (FL): StatPearls; 2019.
[2] Papin A, Le Gouill S, and Chiron D (2018). Rationale for targeting tumor cells in their microenvironment for mantle cell lymphoma treatment. *Leuk Lymphoma* **59**, 1064–1072.
[3] Body S, Esteve-Arenys A, Miloudi H, Recasens-Zorzo C, Tchakarska G, Moros A, Bustany S, Vidal-Crespo A, Rodriguez V, and Lavigne R, et al (2017). Cytoplasmic cyclin D1 controls the migration and invasiveness of mantle lymphoma cells. *Sci Rep* **7**, 13946.
[4] Jares P, Colomer D, and Campo E (2012). Molecular pathogenesis of mantle cell lymphoma. *J Clin Invest* **122**, 3416–3423.
[5] Ek S, Dictor M, Jerkeman M, Jirstrom K, and Borrebaeck CA (2008). Nuclear expression of the non B-cell lineage Sox11 transcription factor identifies mantle cell lymphoma. *Blood* **111**, 800–805.
[6] Martin-Garcia D, Navarro A, Valdes-Mas R, Clot G, Gutierrez-Abril J, Prieto M, Ribera-Cortada I, Woroniecka R, and Rymkiewicz G (2019). Susanne Bens, et al., CCND2 and CCND3 hijack immunoglobulin light-chain enhancers in cyclin D1(--) mantle cell lymphoma. *Blood* **133**, 940–951.
[7] Swerdlow SH, Campo E, Pileri SA, Harris NL, Stein H, Siebert R, Advani R, Ghielmini M, Salles GA, and Zelenetz AD, et al (2016). The 2016 revision of the World Health Organization classification of lymphoid neoplasms. *Blood* **127**, 2375–2390.
[8] Bea S, Valdes-Mas R, Navarro A, Salaverria I, Martin-Garcia D, Jares P, Giné E, Pinyol M, Royo C, and Nadeu F, et al (2013). Landscape of somatic mutations and clonal evolution in mantle cell lymphoma. *Proc Natl Acad Sci U S A* **110**, 18250–18255.
[9] Greiner TC, Dasgupta C, Ho VV, Weisenburger DD, Smith LM, Lynch JC, Vose JM, Fu K, Armitage JO, and Braziel RM, et al (2006). Mutation and genomic deletion status of ataxia telangiectasia mutated (ATM) and p53 confer specific gene expression profiles in mantle cell lymphoma. *Proc Natl Acad Sci U S A* **103**, 2352–2357.
[10] Kridel R, Meissner B, Rogic S, Boyle M, Telenius A, Woolcock B, Gunawardana J, Jenkins C, Cochrane C, and Ben-Neriah S, et al (2012). Whole transcriptome sequencing reveals recurrent NOTCH1 mutations in mantle cell lymphoma. *Blood* **119**, 1963–1971.
[11] Chen Y, Zhao B, Zhu Y, Zhao H, and Ma C (2019). HIF-1-VEGF-Notch mediates angiogenesis in temporomandibular joint osteoarthritis. *Am J Transl Res* **11**, 2969–2982.
[12] Huang T, Sun L, Yuan X, and Qiu H (2017). Thrombospondin-1 is a multifaceted player in tumor progression. *Oncotarget* **8**, 84546–84558.
[13] Ousset M, Bouquet F, Fallone F, Biard D, Dray C, Valet P, Salles B, and Muller C (2010). Loss of ATM positively regulates the expression of hypoxia inducible factor 1 (HIF-1) through oxidative stress: Role in the physiopathology of the disease. *Cell Cycle* **9**, 2814–2822.
[14] Eskelund CW, Dahl C, Hansen JW, Westman M, Kolstad A, Pedersen LB, Montano-Almendras CP, Husby S, Freiburghaus C, and Ek S, et al (2017). TP53 mutations identify younger mantle cell lymphoma patients who do not benefit from intensive chemoimmunotherapy. *Blood* **130**, 1903–1910.
[15] Baran-Marszak F, Boukhiar M, Harel S, Laguillier C, Roger C, Gressin R, Martin A, Fagard R, Varin-Blank N, and Ajchenbaum-Cymbalista Fe, et al (2010). Constitutive and B-cell receptor-induced activation of STAT3 are important signaling pathways targeted by bortezomib in leukemic mantle cell lymphoma. *Haematologica* **95**, 1865–1872.
[16] Mohanty A, Sandoval N, Phan A, Nguyen TV, Chen RW, Budde E, Mei M, Popplewell L, Pham LV, and Kwak LW, et al (2019). Regulation of SOX11 expression through CCND1 and STAT3 in mantle cell lymphoma. *Blood* **133**, 306–318.
[17] Colotta F, Allavena P, Sica A, Garlanda C, and Mantovani A (2009). Cancer-related inflammation, the seventh hallmark of cancer: links to genetic instability. *Carcinogenesis* **30**, 1073–1081.
[18] Balsas P, Palomero J, Eguileor A, Rodriguez ML, Vegliante MC, Planas-Rigol E, Sureda-Gómez M, Cid MC, Campo E, and Amador V (2017). SOX11 promotes tumor protective microenvironment interactions through CXCR4 and FAK regulation in mantle cell lymphoma. *Blood* **130**, 501–513.
[19] Yang Z, Jiang S, Lu C, Ji T, Yang W, Li T, Lv J, Hu W, Yang Y, and Jin Z (2019). SOX11: friend or foe in tumor prevention and carcinogenesis? *Ther Adv Med Oncol* **1758835919853449**, 11.
[20] Chen YH, Gao J, Fan G, and Peterson LC (2010). Nuclear expression of sox11 is highly associated with mantle cell lymphoma but is independent of t(11;14)(q13;q32) in non-mantle cell B-cell neoplasms. *Mod Pathol* **23**, 105–112.

[21] Palomero J, Vegliante MC, Eguileor A, Rodriguez ML, Balsas P, Martinez D, Campo E, and Amador V (2016). SOX11 defines two different subtypes of mantle cell lymphoma through transcriptional regulation of BCL6. *Leukemia* **30**, 1596–1599.

[22] Petrakis G, Veloza L, Clot G, Gine E, Gonzalez-Farre B, Navarro A, Bea S, Martínez A, Lopez-Guillermo A, and Amador V, et al (2019). Increased tumour angiogenesis in SOX11-positive mantle cell lymphoma. *Histopathology* **75**, 704–714.

[23] Kuo PY, Jatiani SS, Rahman AH, Edwards D, Jiang Z, Ahr K, Perumal D, Leshchenko VV, Brody J, and Shaknovich R, et al (2018). SOX11 augments BCR signaling to drive MCL-like tumor development. *Blood* **131**, 2247–2255.

[24] Palomero J, Vegliante MC, Rodriguez ML, Eguileor A, Castellano G, Planas-Rigol E, Jares P, Ribera-Cortada I, Cid MC, and Campo E, et al (2014). SOX11 promotes tumor angiogenesis through transcriptional regulation of PDGFA in mantle cell lymphoma. *Blood* **124**, 2235–2247.

[25] Vegliante MC, Palomero J, Perez-Galan P, Roue G, Castellano G, Navarro A, Clot G, Moros A, Suárez-Cisneros H, and Beà S, et al (2013). SOX11 regulates PAX5 expression and blocks terminal B-cell differentiation in aggressive mantle cell lymphoma. *Blood* **121**, 2175–2185.

[26] Tamma R, Ingravallo G, Albano F, Gaudio F, Annese T, Ruggieri S, Lorusso L, Errede M, Maiorano E, and Specchia G, et al (2019). STAT-3 RNAscope determination in human diffuse large B-cell lymphoma. *Transl Oncol* **12**, 545–549.

[27] Nowak-Sliwinska P, Alitalo K, Allen E, Anisimov A, Aplin AC, Auerbach R, Augustin HG, Bates DO, van Beijnum JR, and Bender RHF, et al (2018). Consensus guidelines for the use and interpretation of angiogenesis assays. *Angiogenesis* **21**, 425–532.

[28] Reale A, Melaccio A, Lamanuzzi A, Saltarella I, Dammacco F, Vacca A, and Ria R (2016). Functional and biological role of endothelial precursor cells in tumour progression: a new potential therapeutic target in haematological malignancies. *Stem Cells Int* **2016**, 7954580.

[29] Liu Y, Beyer A, and Aebersold R (2016). On the dependency of cellular protein levels on mRNA abundance. *Cell* **165**, 535–550.

[30] Kimura Y, Sato K, Imamura Y, Arakawa F, Kiyasu J, Takeuchi M, Miyoshi H, Yoshida M, Niino D, and Sugita Y, et al (2011). Small cell variant of mantle cell lymphoma is an indolent lymphoma characterized by bone marrow involvement, splenomegaly, and a low Ki-67 index. *Cancer Sci* **102**, 1734–1741.

[31] Salar A, Juanpere N, Bellosillo B, Domingo-Domenech E, Espinet B, Seoane A, Romagosa V, Gonzalez-Barca E, Panades A, and Pedro C, et al (2006). Gastrointestinal involvement in mantle cell lymphoma: a prospective clinic, endoscopic, and pathologic study. *Am J Surg Pathol* **30**, 1274–1280.

[32] Nygren L (2012). S Baumgartner Wennerholm, M Klimkowska, B Christensson, E Kimby and B Sander, Prognostic role of SOX11 in a population-based cohort of mantle cell lymphoma. *Blood* **119**, 4215–4223.

[33] Nordstrom L, Andreasson U, Jerkeman M, Dictor M, Borrebaeck C, and Ek S (2012). Expanded clinical and experimental use of SOX11 — using a monoclonal antibody. *BMC Cancer* **12**, 269.

[34] Wang M, Zhao J, Zhang L, Wei F, Lian Y, Wu Y, Gong Z, Zhang S, Zhou J, and Caoet K, et al (2017). Role of tumor microenvironment in tumorigenesis. *J Cancer* **8**, 761–773.

[35] Chen F, Zhuang X, Lin L, Yu P, Wang Y, Shi Y, Hu G, and Sun Y (2015). New horizons in tumor microenvironment biology: challenges and opportunities. *BMC Med* **13**, 45.

[36] Medinger M, Fischer N, and Tzankov A (2010). Vascular endothelial growth factor-related pathways in hemato-lymphoid malignancies. *J Oncol* **2010**, 729725.

[37] Ribatti D, Nico B, Ranieri G, Specchia G, and Vacca A (2013). The role of angiogenesis in human non-Hodgkin lymphomas. *Neoplasia* **15**, 231–238.

[38] Petrakis G, Veloza L, Clot G, Gine E, Gonzalez-Farre B, Navarro A, Bea S, Martínez A, Lopez-Guillermo A, and Amador V, et al (2019). Increased tumour angiogenesis in SOX11-positive mantle cell lymphoma. *Histopathology* .

[39] Siemerink MJ, Klaassen I, Vogels IM, Griffioen AW, Van Noorden CJ, and Schlingemann RO (2012). CD34 marks angiogenic tip cells in human vascular endothelial cell cultures. *Angiogenesis* **15**, 151–163.

[40] Nygren L, Wasik AM, Baumgartner-Wennerholm S, Jeppsson-Ahlberg A, Klimkowska M, Andersson P, Buhrkuhl D, Christensson B, Kimby E, and Wahlinet BE, et al (2014). T-cell levels are prognostic in mantle cell lymphoma. *Clin Cancer Res* **20**, 6096–6104.

[41] Zhang XY, Xu J, Zhu HY, Wang Y, Wang L, Fan L, and Wu YJ (2016). JY Li and Wei Xu, Negative prognostic impact of low absolute CD4(+) T cell counts in peripheral blood in mantle cell lymphoma. *Cancer Sci* **107**, 1471–1476.

[42] He LY, Li L, Guo ML, Zhang Y, and Zhang HZ (2015). Relationship between CD4+CD25+ Treg and expression of HIF-1alpha and Ki-67 in NSCLC patients. *Eur Rev Med Pharmacol Sci* **19**, 1351–1355.

[43] Baraka A and Salem HM (2011). Clinical significance of T-regulatory cells in B-cell non-Hodgkin's lymphoma. *Egypt J Immunol* **18**, 23–30.

[44] Catakovic K, Gassner FJ, Ratswohl C, Zaborsky N, Rebhandl S, Schubert M, Steiner M, Gutjahr J Christine, Pleyer L, and Egle A, et al (2017). TIGIT expressing CD4+T cells represent a tumor-supportive T cell subset in chronic lymphocytic leukemia. *Oncoimmunology* 7e1371399.

[45] Yang F, Wei Y, Cai Z, Yu L, Jiang L, Zhang C, Yan H, Wang Q, Cao X, and Liang T, et al (2015). Activated cytotoxic lymphocytes promote tumor progression by increasing the ability of 3LL tumor cells to mediate MDSC chemoattraction via Fas signaling. *Cell Mol Immunol* **12**, 66–76.

[46] Cai Z, Yang F, Yu L, Yu Z, Jiang L, Wang Q, Yang Y, Wang L, Cao X, and Wang J (2012). Activated T cell exosomes promote tumor invasion via Fas signaling pathway. *J Immunol* **188**, 5954–5961.

[47] Choi K, Benveniste EN, and Choi C (2003). Induction of intercellular adhesion molecule-1 by Fas ligation: proinflammatory roles of Fas in human astroglioma cells. *Neurosci Lett* **352**, 21–24.

[48] Burger JA and Ford RJ (2011). The microenvironment in mantle cell lymphoma: cellular and molecular pathways and emerging targeted therapies. *Semin Cancer Biol* **21**, 308–312.

[49] Papin A, Tessoulin B, Bellanger C, Moreau A, Le Bris Y, Maisonneuve H, Moreau P, Touzeau C, Amiot M, and Pellat-Deceunynck C, et al (2019). CSF1R and BTK inhibitions as novel strategies to disrupt the dialog between mantle cell lymphoma and macrophages. *Leukemia* **33**, 2442–2453.

[50] Barros MH, Hauck F, Dreyer JH, Kempkes B, and Niedobitek G (2013). Macrophage polarisation: an immunohistochemical approach for identifying M1 and M2 macrophages. *PLoS One* **8**e80908.

[51] Barros MH, Hassan R, and Niedobitek G (2012). Tumor-associated macrophages in pediatric classical Hodgkin lymphoma: association with Epstein-Barr virus, lymphocyte subsets, and prognostic impact. *Clin Cancer Res* **18**, 3762–3771.

[52] McWhorter FY, Wang T, Nguyen P, Chung T, and Liu WF (2013). Modulation of macrophage phenotype by cell shape. *Proc Natl Acad Sci U S A* **110**, 17253–17258.

[53] Atri C, Guerfali FZ, and Laouini D (2018). Role of human macrophage polarization in inflammation during infectious diseases. *Int J Mol Sci* **19**.

[54] Corliss BA, Azimi MS, Munson JM, Peirce SM, and Murfee WL (2016). Macrophages: an inflammatory link between angiogenesis and lymphangiogenesis. *Microcirculation* **23**, 95–121.

[55] Federmann B, Frauenfeld L, Pertsch H, Borgmann V, Steinhilber J, Bonzheim I, Fend F, and Quintanilla-Martinez L (2019). Highly sensitive and specific in situ hybridization assay for quantification of SOX11 mRNA in mantle cell lymphoma reveals association of TP53 mutations with negative and low SOX11 expression. *Haematologica* .

[56] Delfau-Larue MH, Klapper W, Berger F, Jardin F, Briere J, Salles G, Casasnovas O, Feugier P, Haioun C, and Ribrag V, et al (2015). High-dose cytarabine does not overcome the adverse prognostic value of CDKN2A and TP53 deletions in mantle cell lymphoma. *Blood* **126**, 604–611.

[57] Uehara I and Tanaka N (2018). Role of p53 in the regulation of the inflammatory tumor microenvironment and tumor suppression. *Cancers (Basel)* **10**.

[58] Yared MA, Khoury JD, Medeiros LJ, Rassidakis GZ, and Lai R (2005). Activation status of the JAK/STAT3 pathway in mantle cell lymphoma. *Arch Pathol Lab Med* **129**, 990–996.

[59] Zhang L, Yang J, Qian J, Li H, Romaguera JE, Kwak LW, Wang M, and Yi Q (2012). Role of the microenvironment in mantle cell lymphoma: IL-6 is an important survival factor for the tumor cells. *Blood* **120**, 3783–3792.

[60] Rudelius M, Rosenfeldt MT, Leich E, Rauert-Wunderlich H, Solimando AG, Beilhack A, Ott G, and Rosenwald A (2018). Inhibition of focal adhesion kinase overcomes resistance of mantle cell lymphoma to ibrutinib in the bone marrow microenvironment. *Haematologica* **103**, 116–125.

[61] Solimando AG, Ribatti D, Vacca A, and Einsele H (2016). Targeting B-cell non Hodgkin lymphoma: New and old tricks. *Leuk Res* **42**, 93–104.

[62] Tam CS, Anderson MA, Pott C, Agarwal R, Handunnetti S, Hicks RJ, Burbury K, Turner G, Di Iulio J, and Bressel M, et al (2018). Ibrutinib plus venetoclax for the treatment of mantle-cell lymphoma. *N Engl J Med* **378**, 1211–1223.